Electronic Supplementary Material (ESI) for Journal of Materials Chemistry A.
This journal is © The Royal Society of Chemistry 2020

Supplementary Information

Scalable Microgel Spinning of Three-Dimensional Porous Graphene Fiber for High-Performance Flexible Supercapacitors

Wujun Ma,[ab] Wanfei Li, *[c] Min Li, [a] Qinghui Mao,[a] Zhenghui Pan,[d] Meifang Zhu,*[b] Yuegang Zhang*[e]

[a] College of Textile and Garment, Nantong University, Nantong 226019, China

[b] College of Materials Science and Engineering, Donghua University, Shanghai 201620, China

[c] Research Center for Nanophotonic and Nanoelectronic Materials, School of Materials Science and Engineering, Suzhou University of Science and Technology, Suzhou 215009, China

[d] Department of Materials Science and Engineering, National University of Singapore, Singapore 117574, Singapore

[e] Department of Physics, Tsinghua University, Beijing 100084, China

*E-mail: yuegang.zhang@tsinghua.edu.cn; wfli2018@mail.usts.edu.cn; zhumf@dhu.edu.cn

Figure and Table list:

Table S3 Comparison of electrochemical properties of various carbon based fiber supercapacitors.

1. Materials and Methods

Preparation of GO microhydrogel Spinning Dopes. GO was prepared by a modified Hummers' method, as previously described. In a typical procedure, the prepared GO was sonicated in water to give a homogeneous aqueous dispersion with a concentration of 3 mg ml^{-1}. Then 20 ml of GO dispersion was mixed with 300 mg allylthiourea in a 30 ml cylindrical glass vial. After being sonicated for 5 minutes, the mixture was then placed in a 95 °C oven for 40 minutes to obtain GO microhydrogel. Then the obtained GO microhydrogel was centrifuged at 5,000 rpm for 20 minutes. After pouring out the supernatant, 1 ml GO dispersion was mixed with the GO microhydrogel. After being vigorously shaken for 10 minutes, the mixture was centrifuged at 10,000 rpm for 10 minutes to obtain the spinning dopes.

Preparation of NS-GF. The NS-GF was fabricated using a home-made spinning equipment. For a typical procedure, the obtained GO microhydrogel spinning dopes was injected into a rotating acetic acid coagulation bath, the injection rate was 30 μl /minute and the coagulation bath rotated at speeds 8 rpm, the gel fiber was direct collected onto a roller and then dried at 60 °C for 12 h. Finally, the dried fiber was reduced at 650 °C for 2 h in argon atmosphere.

Materials Characterization. The morphologies of the fibers were characterized by a scanning electron microscope (HITACHI, S4800). The electrical conductivity of the fibers was measured by two-probe resistance tester. Tensile tests were carried out at an extension rate of 2 mm min^{-1} with a gauge length of 10 mm on a XQ-1A fiber tension tester (Shanghai New Fiber Instrument). Nitrogen sorption isotherms were measured using Micromeritics ASAP2020. Raman spectroscopy measurements were performed using a Renishaw Via laser micro-Raman system at an excitation wavelength of 514 nm. The X-ray photoelectron spectra

(XPS) were obtained on an Axis Ultra DLD spectrometer (Kratos Analytical, UK) using a monochromatic Al K source.

Electrochemical characterization.

Individual fiber electrode: The fiber electrode was prepared by connecting a fiber to stainless steel strip end to end by silver paste. Electrochemical tests were performed using a three-electrode configuration on an electrochemical workstation (CHI 660E) in 1M H_2SO_4 electrolyte. Fiber electrode was used as working electrode, a Pt wire and Hg/Hg_2SO_4 electrode were used as the counter and reference electrode, respectively. The capacitance was calculated from GCD curves using the equation:

$$C = \frac{I\,\Delta t}{\Delta U} \tag{1}$$

where C is the total capacitance, I and Δt are the discharging current and time, respectively, and ΔU is the potential window after IR drop.

The volumetric capacitances (C_V) was calculated according to the equation:

$$C_V = \frac{C}{V} \tag{2}$$

where V refer to the volume of the fiber electrode. The calculation of V is according to the equation

$$V = \pi R^2 L \tag{3}$$

where R is the radius of the fiber, L is the fiber length.

Fiber-Shaped SCs: The H_2SO_4/PVA gel electrolyte was prepared as follows: PVA (3.0 g) was added to 27.0 g deionized water, followed by heating at 95 °C under magnetic stirring until the solution became clear. H_2SO_4 (3.0 g) was finally dropped to the above solution to form the gel electrolyte. To fabricate a fiber-based SCs, two fibers with the same diameter and length (1cm) were connected to a metal wire by Ag paste, respectively, immersed in the H_2SO_4/PVA gel solution for 24 h, dried at

room temperature until the gel electrolyte solidified, and then carefully twisted together to produce a fiber-based SC.

The electrochemical performances of the fiber-shaped SC were evaluated using a two-electrode configuration on an electrochemical workstation (CHI 660E). The capacitance of the supercapacitor was calculated from its discharge curves using

$$C = \frac{I\,\Delta t}{\Delta U} \tag{4}$$

where C is the total capacitance, I and Δt are the discharging current and time, respectively, and ΔU is the potential window after IR drop.

The volumetric capacitances (C_V) of the device was calculated using the equations

$$C_V = \frac{C}{2V} \tag{5}$$

where V refers to the volume of one fiber in the device.

The volumetric energy (E_V) and power (P_V) density of the device was obtained from the equation

$$E_V = \frac{1}{2} C_V\,\Delta U^2 \tag{6}$$

$$P_V = E_V / t_{discharge} \tag{7}$$

2. Supplementary Figures

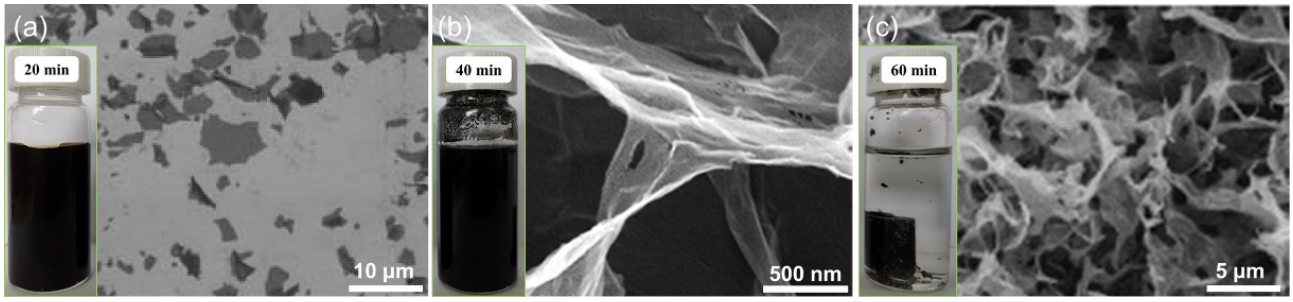

Figure S1 Optical images of GO self-assembly process at different reduction time (Inset) and their corresponding SEM images.

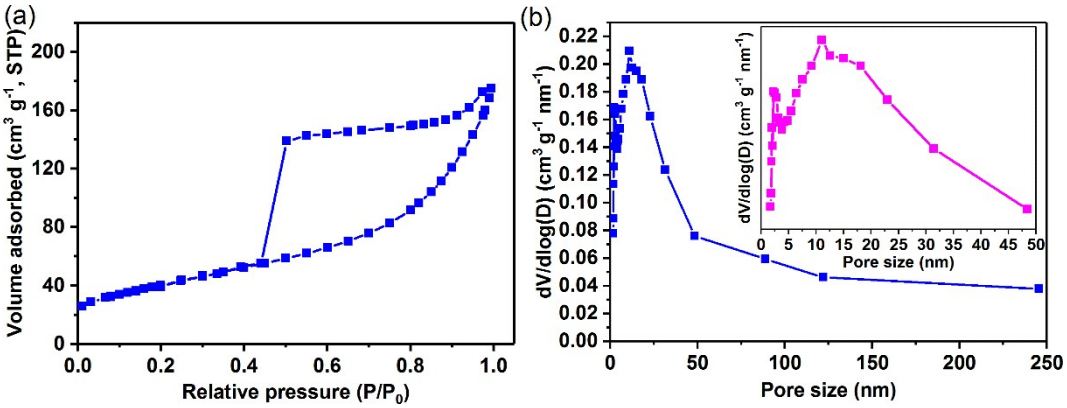

Figure S2 (a) N_2 adsorption–desorption isotherms of NS-GF. (b) Pore size distributions of NS-GF.

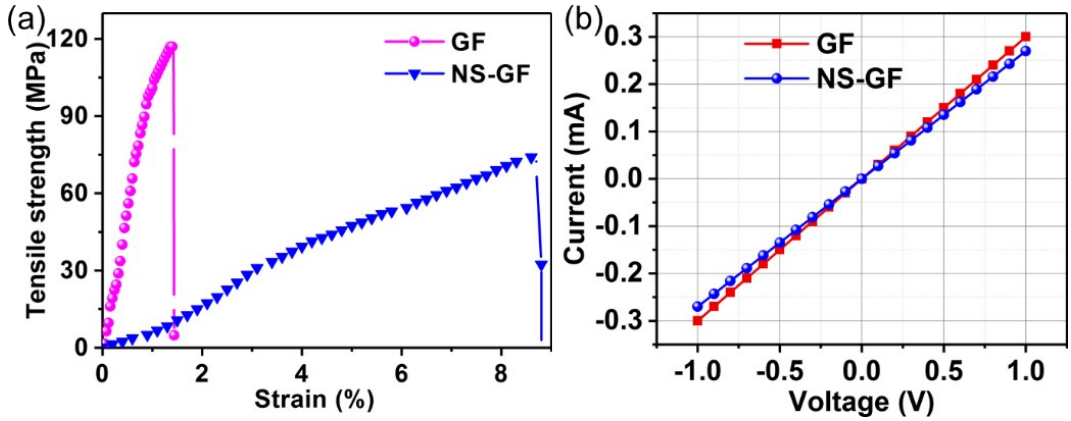

Figure S3 Stress-strain (a) and I-V curves (b) of GF and NS-GF.

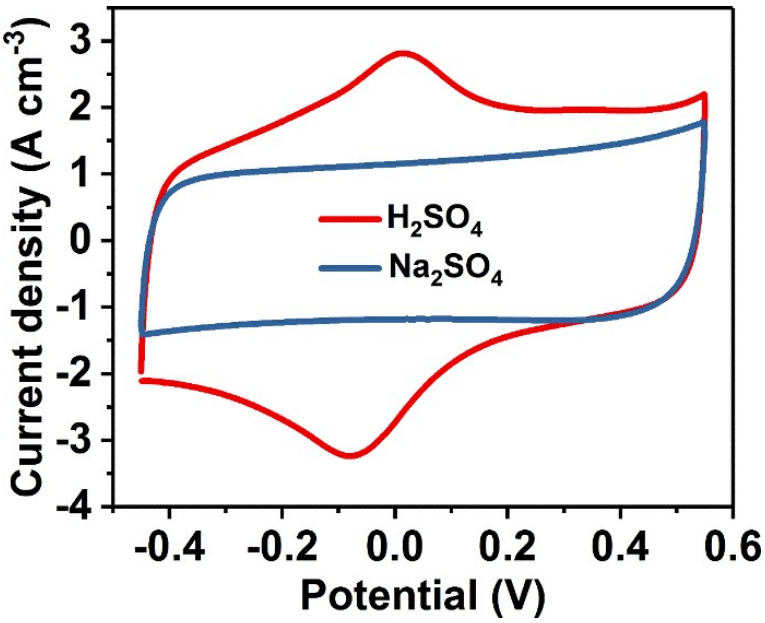

Figure S4 Cyclic voltammetry curves of the NS-GF in 1M H_2SO_4 and 1M Na_2SO_4.

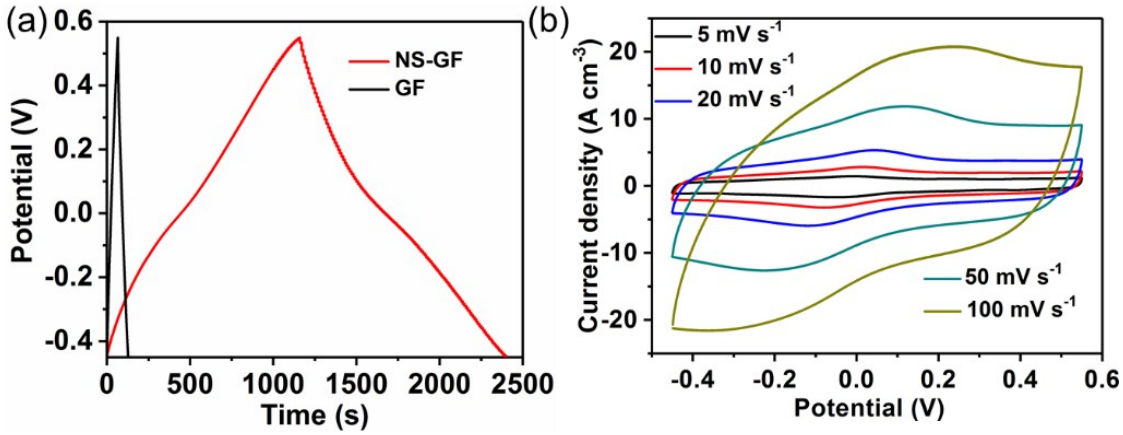

Figure S5 (a) Galvanostatic charge/discharge curves of the GF and NS-GF at a current density of 0.2 A cm^{-3}. (b) Cyclic voltammetry curves of the NS-GF at various scan rates.

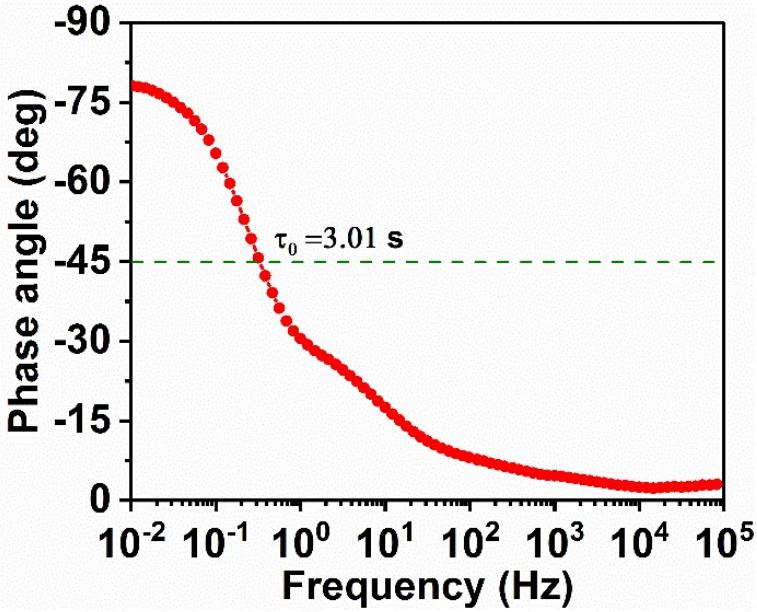

Figure S6 Bode phase plot of NS-GF.

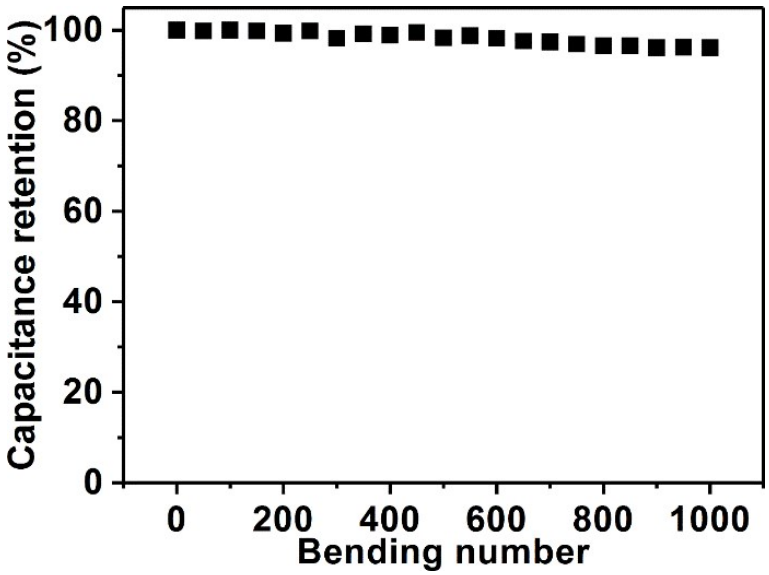

Figure S7 Capacitance retention during 1000 bending cycles between a bending angle of 0^{o} and 180^{o}.

Figure S8 Optical image of an electronic watch powered by a charged device connected in series.

3. Supplementary Table

Table S1 Coulombic efficiency of the all-solid-state supercapacitor at different current density.

Current density (mA cm^{-3})	100	150	200	300	500	1000
Coulombic efficiency	78.5%	83.3%	87.8%	95.4%	92.1%	91.8%

Table S2 Electrochemical properties of the all-solid-state supercapacitor.

	C	E	P
V	59.9 Fcm^{-3}	8.3 mWh cm^{-3}	1048.4 mW cm^{-3}
S	49.9 mF cm^{-2}	6.9 μWh cm^{-2}	870 μW cm^{-2}
L	599 μF cm^{-1}	83 μWh cm^{-1}	100 μW cm^{-1}
M	133.1 F g^{-1}	18.4 mWh g^{-1}	2.3 W g^{-1}

V, S, L and M are the volume, surface area, length and mass of two electrodes.

Table S3 Comparison of electrochemical properties of various carbon based fiber supercapacitors.

Ref.	Materials	Electrolyte	C_V F cm^{-3}	P_V mW cm^{-3}	E_V mWh cm^{-3}
[1]	CNT/Carbon fiber	PVA/H_3PO_4	-	2.7	0.14
[2]	CNT sheet/CNT fiber	PVA/H_3PO_4	32.09	-	-
[3]	MnO_2/CNT fiber	$LiPF_6$	-	790	1.7
[4]	MnO_2/Carbon fiber	PVA/H_3PO_4	2.5	400	0.22
[5]	ZnO/MnO_2/Carbon fiber	PVA/LiCl	-	2.4	0.04
[6]	PPy/MnO_2/Carbon fiber	PVA/H_3PO_4	69.6	2000	6.16
[7]	PEDOT/MWCNT/Pt wire	PVA/H_2SO_4	-	40000	1.4
[8]	PEDOT/RGO fiber	PVA/H_3PO_4	78.8	-	7.0
[9]	MnO_2@MWCNT fiber	PVA/LiCl	8.5	2500	1.5
[10]	CNT/MnO_2 fiber	PVA/KOH	25.4	127	3.52
[11]	MoS_2 rGO/MWCNT fiber	PVA/H_2SO_4	5.2	2300	0.97
[12]	RGO+CNT@CMC	PVA/H_3PO_4	39.5	18	3.5
[13]	RGO+CNT	PVA/H_3PO_4	38.8	700	3.4
[14]	SWCNT@C	PVA/H_2SO_4	12.1	3840	3.7
This work	NS-GF	PVA/ H_2SO_4	59.9	1048.4	8.3

REFERENCES

[1] V. T. Le, H. Kim, A. Ghosh, J. Kim, J. Chang, Q. A. Vu, D. T. Pham, J.-H. Lee, S.-W. Kim, Y. H. Lee, *ACS Nano* **2013**, *7*, 5940.

[2] X. L. Chen, L. B. Qiu, J. Ren, G. Z. Guan, H. J. Lin, Z. T. Zhang, P. N. Chen, Y. G. Wang, H. S. Peng, *Adv. Mater.* **2013**, *25*, 6436.

[3] J. Ren, L. Li, C. Chen, X. L. Chen, Z. B. Cai, L. B. Qiu, Y. G. Wang, X. R. Zhu, H. S. Peng, *Adv. Mater.* **2013**, *25*, 1155.

[4] X. Xiao, T. Li, P. Yang, Y. Gao, H. Jin, W. Ni, W. Zhan, X. Zhang, Y. Cao, J. Zhong, L. Gong, W.-C. Yen, W. Mai, J. Chen, K. Huo, Y.-L. Chueh, Z. L. Wang, J. Zhou, *ACS Nano* **2012**, *6*, 9200.

[5] P. Yang, X. Xiao, Y. Li, Y. Ding, P. Qiang, X. Tan, W. Mai, Z. Lin, W. Wu, T. Li, H. Jin, P. Liu, J. Zhou, C. P. Wong, Z. L. Wang, *ACS Nano* **2013**, *7*, 2617.

[6] J. Tao, N. Liu, W. Ma, L. Ding, L. Li, J. Su, Y. Gao, *Sci. Rep.* **2013**, *3*, 2286.

[7] J. A. Lee, M. K. Shin, S. H. Kim, H. U. Cho, G. M. Spinks, G. G. Wallace, M. D. Lima, X. Lepró, M. E. Kozlov, R. H. Baughman, S. J. Kim, *Nat. Commun.* **2013**, *4*, 1970.

[8] S. Padmajan Sasikala, K. E. Lee, J. Lim, H. J. Lee, S. H. Koo, I. H. Kim, H. J. Jung, S. O. Kim, *ACS Nano* **2017**, *9*, 9424.

[9] P. Shi, L. Li, L. Hua, Q. Qian, P. Wang, J. Zhou, G. Sun, W. Huang, *ACS Nano* **2017**, *11*, 444.

[10] C. Choi, J. A. Lee, A. Y. Choi, Y. T. Kim, X. Lepró, M. D. Lima, R. H. Baughman, S. J. Kim, *Adv. Mater.* **2014**, *26*, 2059.

[11] G. Sun, X. Zhang, R. Lin, J. Yang, H. Zhang, P. Chen, *Angew. Chem., Int. Ed.* **2015**, *127*, 4734.

[12] L. Kou, T. Huang, B. Zheng, Y. Han, X. Zhao, K. Gopalsamy, H. Sun, C. Gao, *Nat. Commun.* **2014**, *5*, 3754.

[13] Y. Ma, P. Li, J. W. Sedloff, X. Zhang, H. Zhang, J. Liu, *ACS Nano* **2015**, *9*, 1352.

[14] Q. Meng, H. Wu, Y. Meng, K. Xie, Z. Wei, Z. Guo, *Adv. Mater.* **2014**, *26*, 4100.